 doi:10.20944/preprints202011.0465.v1

*Article*

# Web Unevenness due to Thermal Deformation in Roll – to – Roll Manufacturing Process

**Minho Jo [1], Jongsu Lee [2], Seongyong Kim [3], Gyoujin Cho [4] , Taik-min Lee [5] and Changwoo Lee [6,*]**

[1] Department of Mechanical Design and Production Engineering, Konkuk University, 120 Neungdong-ro, Gwangjin-gu, Seoul 05030, Korea; rnjstk1234@gmail.com
[2] Department of Printed Electronics Engineering, Sunchon National University ,225, Jungang-ro, Suncheon 57922, Korea; ljs8755@gmail.com
[3] Department of Mechanical Design and Production Engineering, Konkuk University, 120 Neungdong-ro, Gwangjin-gu, Seoul 05030, Korea; arsen6788@gmail.com
[4] Institute of Quantum Biophysics.,Sungkyukwan University, 2066 Seobu-ro, Jangan-gu, Suwon 16419, Korea; gcho1004@skku.edu
[5] Korea Institute of Machinery and Materials(KIMM), Intelligence and Precision Machinery Research Division, 156 Gajeongbuk-ro, Yuseong-gu, Daejeon 34103, Korea; taikmin@kimm.re.kr
[6] Department of Mechanical Engineering, Konkuk University, 120 Neungdong-ro, Gwangjin-gu, Seoul 05030, Korea
* Correspondence: leewoo1220@konkuk.ac.kr; Tel.:+82-2-450-3570; Fax: +82-2-454-0428

**Abstract:** In roll-to-roll (R2R) processing, uniformity of the web is a crucial factor that can guarantee high coating quality. To understand web defects due to thermal deformation, we analyzed the effects of web unevenness on the coating quality of an yttria-stabilized zirconia (YSZ) layer, a brittle electrolyte of solid oxide fuel cells (SOFCs). We used finite element analysis to analyze the thermal and mechanical deformations at different drying temperatures. A YSZ layer was also coated using R2R slot-die coating to observe effects of web unevenness on the coating quality. It was seen that web unevenness was generated by thermal deformation due the conduction and convection heat from the dryer. Owing to varying web unevenness with time, the YSZ layer developed cracks. At higher drying temperatures, more coating defects having larger widths were generated. Results indicated that web unevenness at the coating section led to coating defects, which could damage the SOFC and decrease its yield in the R2R process. From this study, we suggest that coating defects, generated by the web unevenness owing to the convection and conduction heat, should be considered for the high-volume production of brittle electrolytes using the R2R process.

**Keywords:** coating defect; electrolyte layer; temperature; thermal deformation; roll-to-roll slot-die coating systems; wrinkle

## 1. Introduction

Roll-to-Roll manufacturing process (named R2R process) is eco-friendly, low-cost, and has the advantage of mass-production, which makes it attractive in manufacturing flexible electronic devices such as thin film transistors and solid oxide fuel cells (SOFCs) [1–5]. Recently, a brittle electrolyte, which is a separator used in SOFCs to transmit oxygen ions, has been coated using this R2R process [6]. A Slot-die coating is one of the best methods for coating a large – area electrolyte using this process. In slot-die coating, ink is supplied at a constant flow rate to the reservoir of the slot die coater, discharged through the coater lip while forming a coating bead and then deposited on the web. The coating quality of the liquid varies accordingly with the distance between the coater lip and web (named coating gap), ink viscosity, surface tension of ink, and surface energy of the substrate [7]. Accordingly, many research groups have studied the effects of the ink properties and coating parameters on the coating quality [8,9]. One of the most important parameters in the R2R process is the uniformity of the web obtained in the transverse direction. As such, the material of the web used to coat the electrolyte should be a thin, flexible and non-breakable plastic film like

 doi:10.20944/preprints202011.0465.v1

polyethylene terephthalate (PET) or polyimide (PI) [10–12]. Moreover, the web can be easily deformed by external forces due to the roll eccentricity and temperature fluctuations of the heater in the dryer during the movement of web, which could deteriorate the coating quality. Therefore, numerous studies on the behavior of the web according to external forces have been conducted.

Ebler et al. [9] developed a mathematical model to express the behavior of tension applied to the web in the R2R process and controlled the web tension disturbances using a load cell and passive dancer. Sakamoto et al. [13] proposed a web tension control method based on proportional-integral (PI) controller and analyzed the tension behavior according to different velocity variations of driven rollers using the developed model. Lynch et al. [14] proposed an efficient web tension estimation method using a nonlinear model-based observer, followed by experimental verifications. Shin et al. [15] experimentally analyzed the web tension behavior in the transverse direction. Lee et al. [16] postulated that the surface roughness of the substrate depends on the web tension disturbances in the R2R process, which affects the coating and printing qualities. Lee et al. [17] analyzed the effects of temperature disturbance in the dryer on the thermal characteristics of the web followed by experimental verifications. Lu et al. [18] studied the behavior of the web according to the heat conducted by the heating rollers in the R2R process.

As mentioned above, in the previous studies, the tension fluctuation in the web due to the velocity variations of driven rollers and temperature disturbances in dryer in the R2R process have been mainly considered. However, few studies have been conducted on the web defects due to the thermal deformation of the dryer inlet [7]. The thermal deformations of the web could generate a sine-wave shaped deformation of the web in the transverse direction (named web unevenness). If such a web unevenness occurs in the coating section, the coating bead may become unstable, and the thickness of the coating layer becomes non-uniform even though desired coating parameters are set. Moreover, a crack could be generated by bending of the coating layer due to the web unevenness if a brittle material is coated on the uneven web. These coating defects can negatively affect the performance of the devices constructed on the coated layer [19, 20]. Therefore, it is essential to study the defects at the inlet of the dryer during the coating of a brittle material to obtain a high - quality electrolyte layer in the R2R process.

In this study, we analyzed the effects of the thermal deformation in the tensioned web and the web unevenness near the inlet of the dryer on the coating quality of a brittle electrolytic layer. First, the behavior of the tensioned web was analyzed according to the drying temperature using finite element analysis (FEA). A finite element model (FEM) was designed considering the boundary conditions and external forces applied to the web near the inlet of the dryer. The simulation results show that the thermal deformation of the web leads to web unevenness, whose amplitude increases with increasing the drying temperature. Finally, yttria-stabilized zirconia (YSZ), an electrolyte of SOFC, was coated by a R2R slot-die coating process at various drying temperatures to clearly observe the effects of the web unevenness on the coating quality of the YSZ layer and the performance of the SOFC fabricated using this layer.

## 2. Finite Element Analysis : Thermal – Structural Coupled Analysis

### *2.1. Finite Element Modeling*

A thermal-structural coupling analysis was carried out using FEA. Considering the boundary conditions at the inlet of the dryer and external forces applied to the web, an FEM of the web near the inlet of the dryer was designed to understand the deformation of the web due to the convection and conduction heats from the dryer. A polyethylene terephthalate (PET) film (CD-901, KORON Inc., Korea) was used in this study. Table 1 presents the mechanical and thermal properties of the web, while the boundary conditions defined for the model are shown in Table. 2

Preprints (www.preprints.org) | NOT PEER-REVIEWED | Posted: 18 November 2020 doi:10.20944/preprints202011.0465.v1

**Table 1.** Mechanical and thermal property of PET flexible substrate.

| Property | Unit | Value |
|---|---|---|
| Density | $kg / m^3$ | 1390 |
| Poisson's ratio | - | 0.33 |
| Young's modulus | $MPa$ | 4800 |
| Specific heat | $J / kg * K$ | 1172 |
| Coefficient of thermal expansion | $K^{-1}$ | 1.7E-05 |

**Table 2.** Boundary Condition used in thermal – structural coupled analysis.

| Physics | Boundary Condition |
|---|---|
| Mechanical | Fixed support |
| Mechanical | Tension |
| Thermal | Drying temperature |
| Thermal | Drying area expansion |

Figure 1(a) indicates the schematics of the web transporting and drying sections in the R2R process. Figures 1(b) and (c) present the enlarged views of the section and tension distribution at the inlet of the dryer indicated by the black -dotted box in Figure 1(a), respectively. In Figure 1(b), x-, y-, and z-directions are taken as the web moving, transverse and web thickness directions, respectively. In Figure 1(a), it can be inferred that the web temperature steadily increases and converges to the drying temperature due to the conduction and convection heats from the dryer as the web is close to the inlet of the dryer. The temperature distribution of the web in the FEM was set considering the temperature distribution at this position. Considering the tension distribution shown in Figure 1(c), boundary conditions at both edges were defined, and set tension was applied to both sides of the web.[21] The drying temperature range was set from 30°C to 120°C considering the temperature range of the actual dryer in the R2R process. 'Solid 226' was used as the element in the FEM to carry out multi-physics coupled analysis using a commercial finite element analysis program (ANSYS Fluent, ANSYS Inc., USA). Equation (1) represents the governing equation to calculate the net thermal deformation in the 'Solid 226' based on the thermal – structural coupled analysis.

$$\{\varepsilon\} = [D]^{-1}\{\sigma\} + \{\alpha\}\Delta T \quad (1)$$

where {ε} is the total strain vector; [D] is the elastic stiffness matrix; {σ} is the vector of coefficients of thermal expansion; ΔT is the temperature variation.

Preprints (www.preprints.org) | NOT PEER-REVIEWED | Posted: 18 November 2020 doi:10.20944/preprints202011.0465.v1

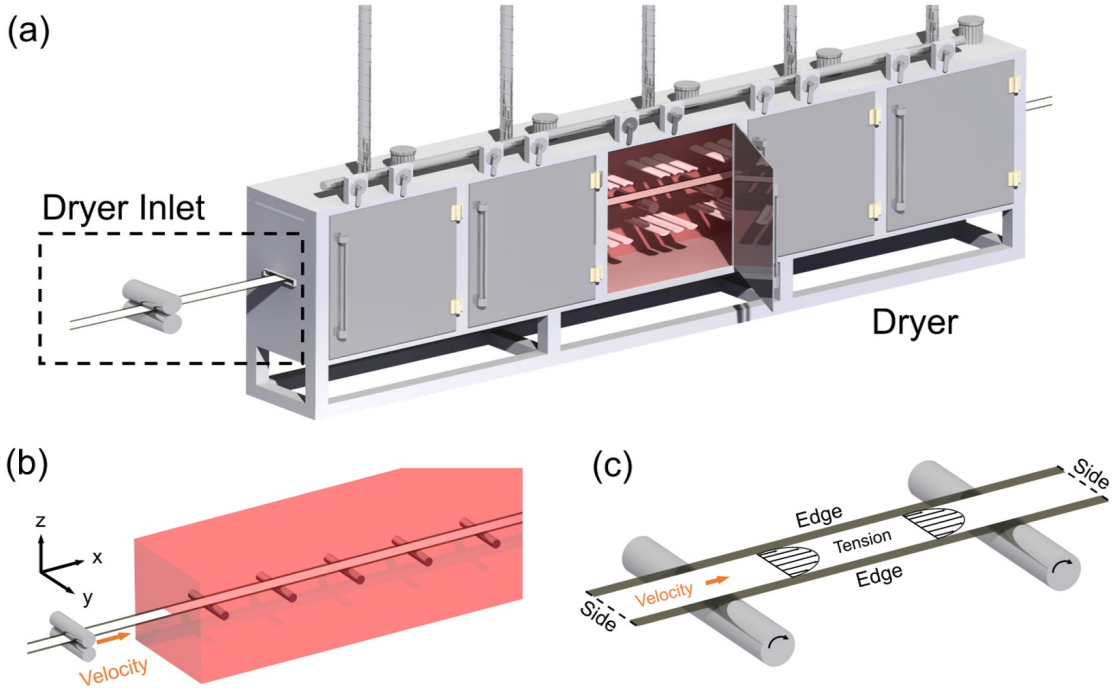


**Figure 1.** Schematic of the flexible substrate in R2R process (a) Dryer (b) Detailed view of dryer inlet (c) Tension distribution on flexible substrate.

*2.2. Simulation Result*

Figure 2 presents the distribution of deformation (unit: mm) in the tensioned web along both y and z directions expressed as contour plots. To plot Figures 2(a)–(d), web speed and tension of 1 m/min and 1 kgf were used, respectively. The drying temperatures were set to 30, 60, 90, and 120 °C. The length of the web model that is, the distance between the slot-die coater and the inlet of the dryer, was 0.5 m in this study. The deformations were magnified 20 times to clearly observe their distributions in the tensioned web according to the drying temperature. The legend at the right of each contour plot shows the web deformation with respect to the color of the contour plot. The white dotted line in all figures represent the inlet of the dryer. In Figure 2(a), one can see that much less deformations in the web occur at the drying temperature of 30 °C than those at 60 °C. The web is compressed by the tensile stress in the transverse direction before the dryer inlet; however, the web expands due to the thermal expansion after passing through the dryer inlet. The thermal deformation in z direction increases more rapidly than those in y direction as the drying temperature increases. Especially, one can clearly see the sine-wave shaped web unevenness after the inlet of the dryer at the 60 °C-drying temperature as shown in Figures 2(a)–(d). Table 3 shows the maximum deformation in the y- and z-directions according to the drying temperature. From the results, one can see that drying temperature dominantly affects the web deformation in the z-direction than in the y-direction. The web unevenness is generated by the thermal deformation caused by the conduction and convection heats from the dryer.

Preprints (www.preprints.org) | NOT PEER-REVIEWED | Posted: 18 November 2020 doi:10.20944/preprints202011.0465.v1

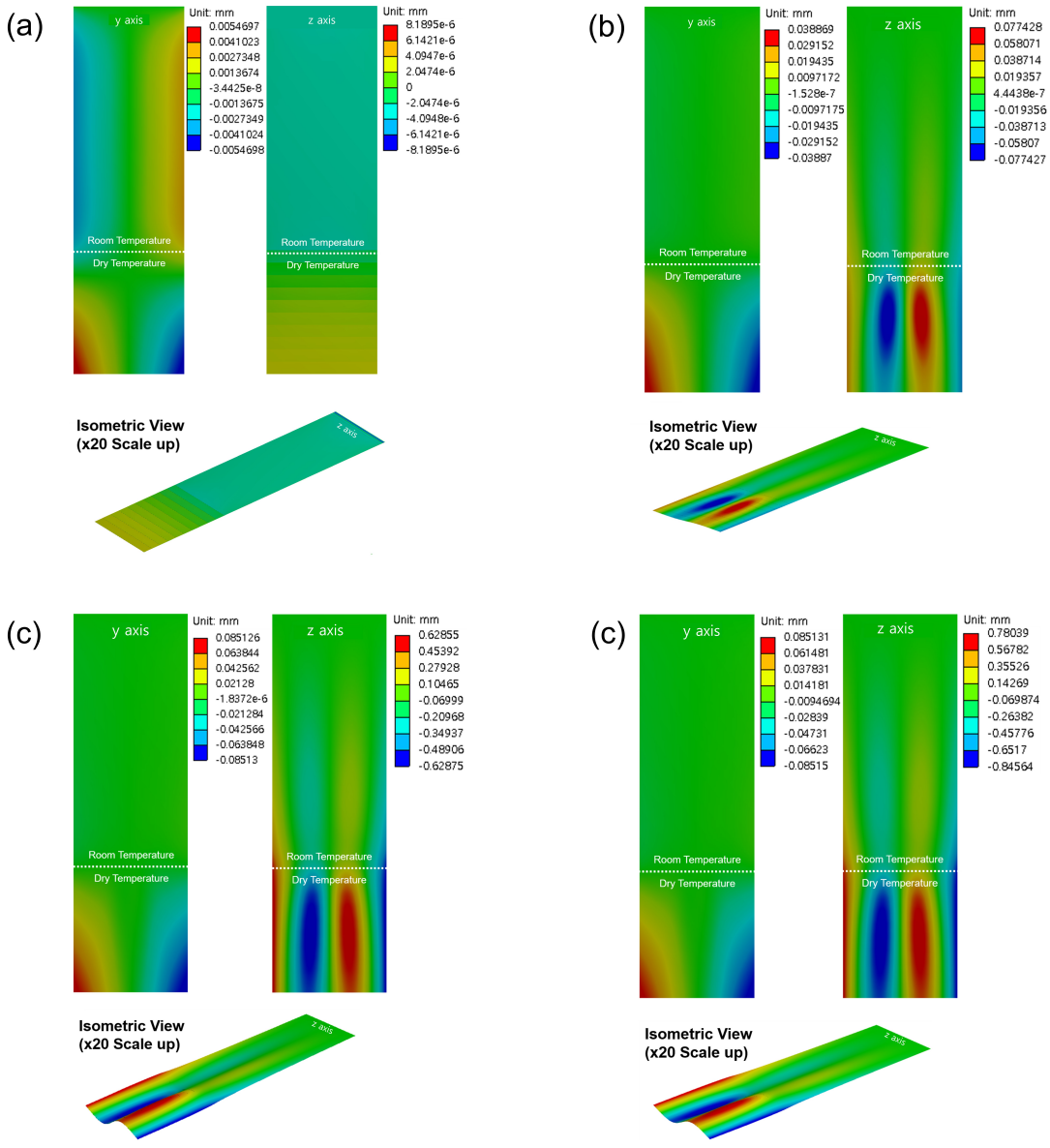


**Figure 2.** Y axis and Z axis deformation behaviors of the flexible substrate at temperatures of: (a) 30°C, (b) 60°C, (c) 90°C, and (d)120°C

**Table 3.** Mechanical and thermal deformations of the PET flexible substrate

| Temperature | Y Deformation (x10$^{-3}$) | Z Deformation (x10$^{-3}$) |
|---|---|---|
| 30°C | 5.4697mm | 0.008mm |
| 60°C | 38.869mm | 77.428mm |
| 90°C | 85.126mm | 628.46mm |
| 120°C | 85.299mm | 780.39mm |

Figure 3 indicates the deformation of the web in y- and z- directions according to the drying temperature. The x- and y-axes of the plots indicate the drying temperature (°C) and web deformation (mm), respectively. It is seen that the deformation in y-direction increases and then remains constant after 90 °C. However, the web deformation in z-direction steadily increases with increasing drying temperatures. Especially, this deformation rapidly increases in the region of the

Preprints (www.preprints.org) | NOT PEER-REVIEWED | Posted: 18 November 2020 doi:10.20944/preprints202011.0465.v1

drying temperature of 60–90 °C. Given that the thermal deformation generates the web unevenness, one can realize that severe web unevenness can occur above a drying temperature of 60 °C. The web unevenness can spread to the coating section, which generates coating defects due to the unstable coating bead and non-uniform web surface.

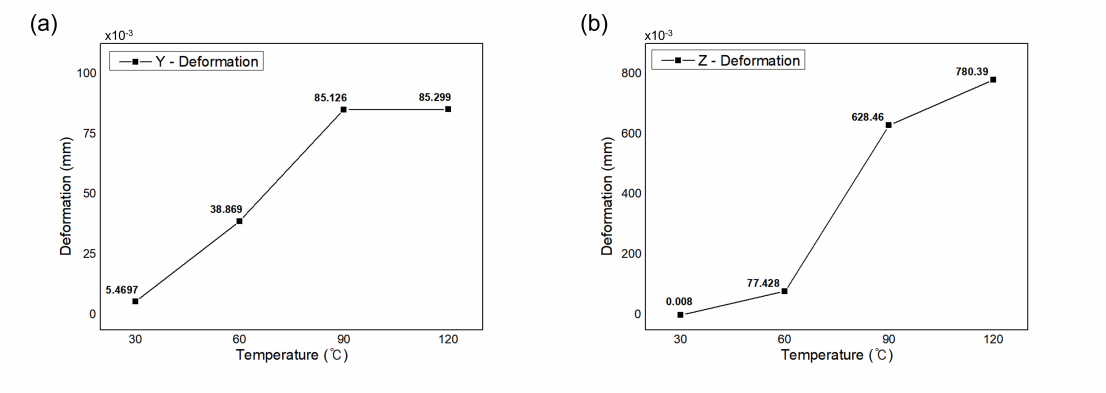


**Figure 3.** Deformation at the temperature domain in the (a) y direction, and (b) z direction.

Figures 4(a) and (b) show the web moving distance according to the web moving time in the dryer and the distribution of the consequent web unevenness. The web speed, tension, and drying temperature are taken as 1 m/min, 1 kgf and 120 °C, respectively. The web unevenness is generated 3.05 s after the web enters the dryer. The amplitudes and positions of the peak and valley of the web unevenness change with respect to the web moving time. Results suggest that the dried brittle layer on which the coating defect occurs is prone to cracking by bending due to the change of the web unevenness according to the web moving time.

Preprints (www.preprints.org) | NOT PEER-REVIEWED | Posted: 18 November 2020 doi:10.20944/preprints202011.0465.v1

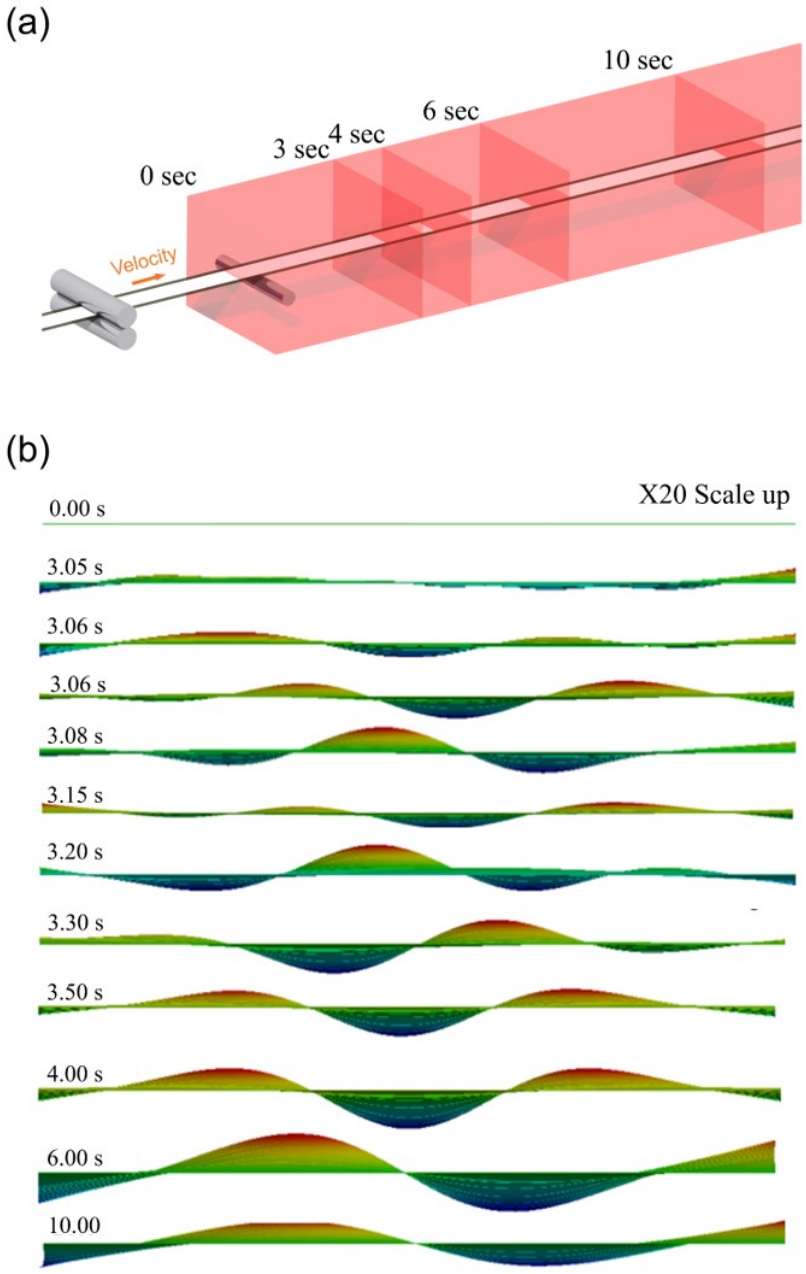


**Figure 4.** (a) Web moving distance over time, and (b) Distribution of the consequent web unevenness (cross-sectional view).

## 3. Experiment

### *3.1. Mechanical Properties of YSZ Coating Layer*

The YSZ electrolyte layer (572349-25G, Sigma-Aldrich Inc., USA) was coated by an industrial-scale R2R slot-die coating machine as shown in Figure 5. The YSZ satisfies the requirements of an electrolyte layer of SOFCs and solid oxide electrolyzer cells (SOECs) due to its advantages of high ion-conductivity and chemical stability [22–25]. Figure 5(a) shows the schematics of R2R slot die coating process and Figure 5(b),(c) shows the enlarged image of the section near the inlet of the dryer. Table 4 lists the properties of YSZ and coating and drying conditions. The coated YSZ layer was separated from the PET film (CD-901, KORON Inc., Korea). The mechanical

Preprints (www.preprints.org) | NOT PEER-REVIEWED | Posted: 18 November 2020 doi:10.20944/preprints202011.0465.v1

properties of the YSZ layer were measured by a tensile tester (Universal Testing System 3345, INSTRON Inc., USA) according to ASTM D882.

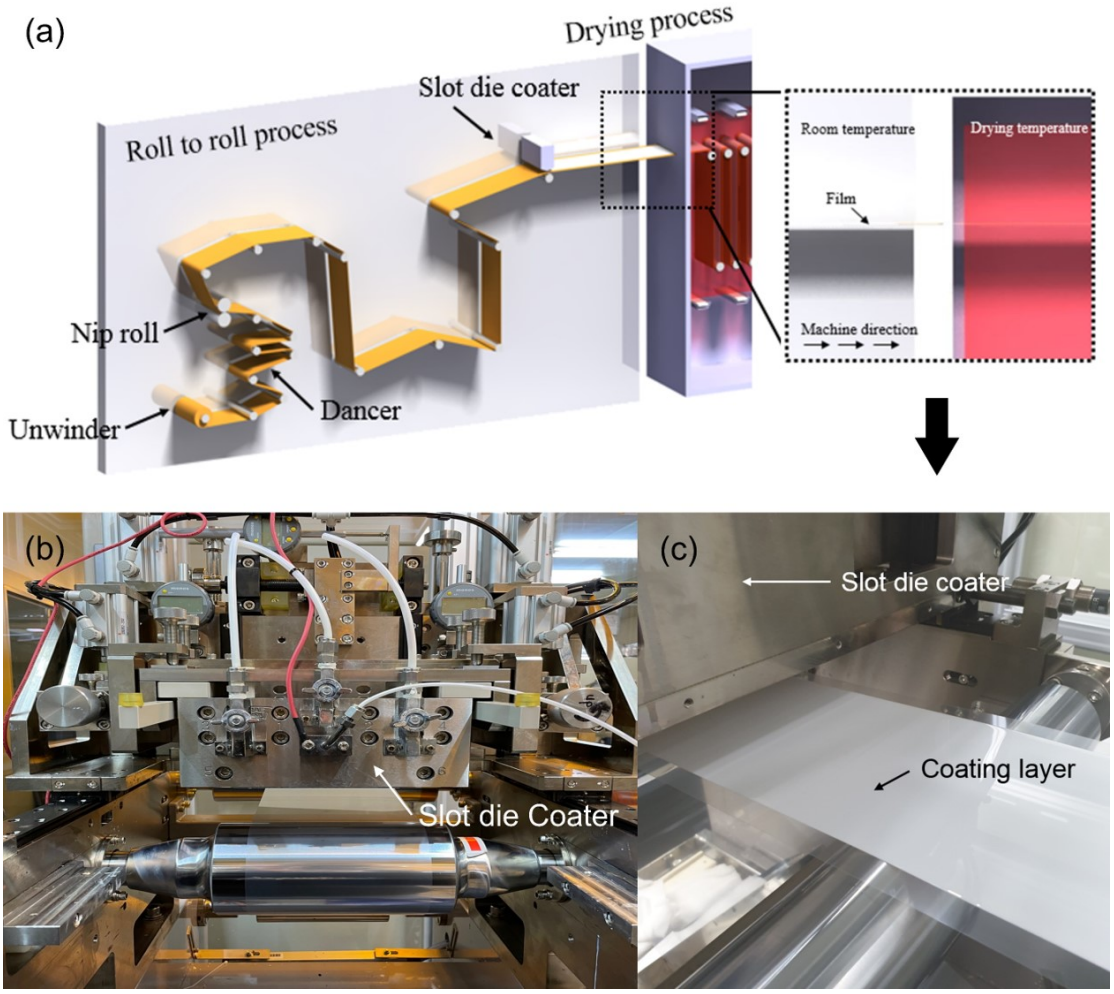


**Figure 5.** (a) Roll – to – roll systems, (b) Slot die coater, and (c) YSZ Layer after coating process.

**Table 4.** YSZ ink properties and processing condition of slot die coating.

| | Properties | Value |
|---|---|---|
| YSZ Ink | Contact Angle (°) | 61.91 |
| | Viscosity (cP) | 30 |
| | Solid contents (%) | 35.91 |
| Substrate | Thickness (mm) | 0.1 |
| | Width (mm) | 150 |
| | Elastic modulus (GPa) | 5.5 |
| | Poisson's ratio | 0.37 |
| Process | Operating tension (kgf) | 1 |
| | Flow rate (ml/min) | 20 |
| | Web speed (mm/min) | 1000 |
| | Coating gap (mm) | 0.35 |
| | Drying temperature (°C) | 30 |

Preprints (www.preprints.org) | NOT PEER-REVIEWED | Posted: 18 November 2020 doi:10.20944/preprints202011.0465.v1

Figures 6(a) and (b) present the behavior of the YSZ layer according to the tensile strain and its stress-strain curve (named s-s curve), respectively. The s-s curve was plotted three times as shown in Figure 6(b). The average tensile stress and strain are found to be 4.84 MPa and 0.329, respectively. One can see that there are few plastic deformation regions in the s-s curves, which suggest that the YSZ layer is very brittle. Our previous study shows that the tensile strain decreased with increasing the drying temperature (0.0088 at 50 °C and 0.0078 at 70 °C) [7].

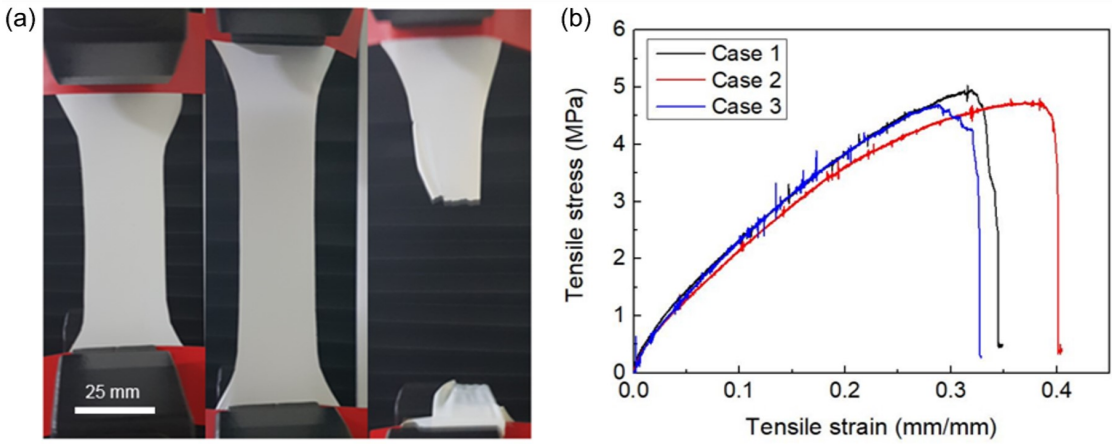


**Figure 6.** (a) YSZ coating layer during the tensile test, and (b) Stress – strain curve.

*3.2. Effects of the web unevenness on the crack in YSZ layer*

The YSZ electrolyte layers were fabricated at four drying temperatures of 30, 60, 90 and 120 °C using the R2R slot-die coating process to analyze the effects of the web unevenness on the crack developed in YSZ layer. Table 5 presents the coating conditions according to the drying conditions. Figures 7(a) and (b) present the dried YSZ layers coated at drying temperatures of 30 °C and 90 °C, respectively. One can see that few coating defects are obtained in the YSZ layer at 30 °C; however, defects in the x-direction are generated in the YSZ layer at 90 °C only. Figure 8 indicates the surface of the YSZ dried at (a–c) 30, (d–f) 60, (g–i) 90, and (j–l) 120 °C measured by a microscope (LV100ND, Nikon, Japan), scanning electron microscope (FE-SEM , S-4800, Hitachi Inc., Japan) and an interferometer (NS-E1000, NanoSystem Co. Ltd., Korea). In Figures 8 (a), (d), (g) and (j), more coating defects are generated at higher drying temperatures. Especially, one can see the defect width also increased with increasing the drying temperature. The web unevenness generated in the dryer is spread to the slot-die coating section, and the YSZ ink coated on the peak of the web unevenness could flow down to the valley as the ink is deposited on the uneven web in the transverse direction, which generates the coating defect. Moreover, the dried layer where the coating defect occurs can be cracked by bending due to the change of the web unevenness during its movement in the dryer. The amplitude and width of the web unevenness below the lip of the slot-die coater is larger at the higher drying temperature as shown in the simulation results in Figure 4, which generates wider coating defects.

Preprints (www.preprints.org) | NOT PEER-REVIEWED | Posted: 18 November 2020 doi:10.20944/preprints202011.0465.v1

**Table 5.** Operating condition of R2R slot die coating process.

| Conditions | Case 1 | Case 2 | Case 3 | Case 4 |
|---|---|---|---|---|
| Film width (mm) | 150 | 150 | 150 | 150 |
| Film thickness (mm) | 0.1 | 0.1 | 0.1 | 0.1 |
| Viscosity of YSZ (cP) | 30 | 30 | 30 | 30 |
| Coating gap (mm) | 0.35 | 0.35 | 0.35 | 0.35 |
| Web speed (mm/min) | 1000 | 1000 | 1000 | 1000 |
| Tension (kgf) | 1 | 1 | 1 | 1 |
| Flow rate (ml/min) | 20 | 20 | 20 | 20 |
| Drying temperature (°C) | 30 | 60 | 90 | 120 |
| Drying time (min) | 5 | 5 | 5 | 5 |

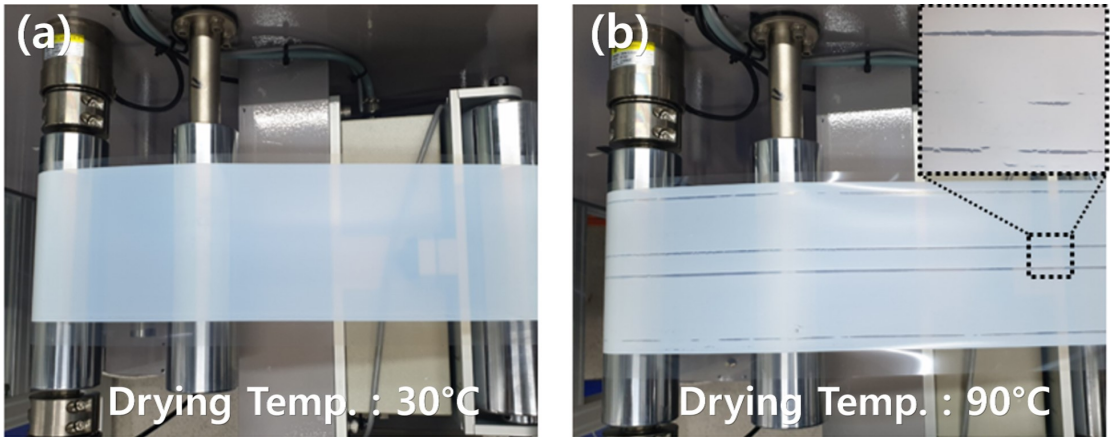


**Figure 7.** YSZ Coating layer dried at (a) 30°C, and (b) 60°C in R2R process.

Preprints (www.preprints.org) | NOT PEER-REVIEWED | Posted: 18 November 2020 doi:10.20944/preprints202011.0465.v1

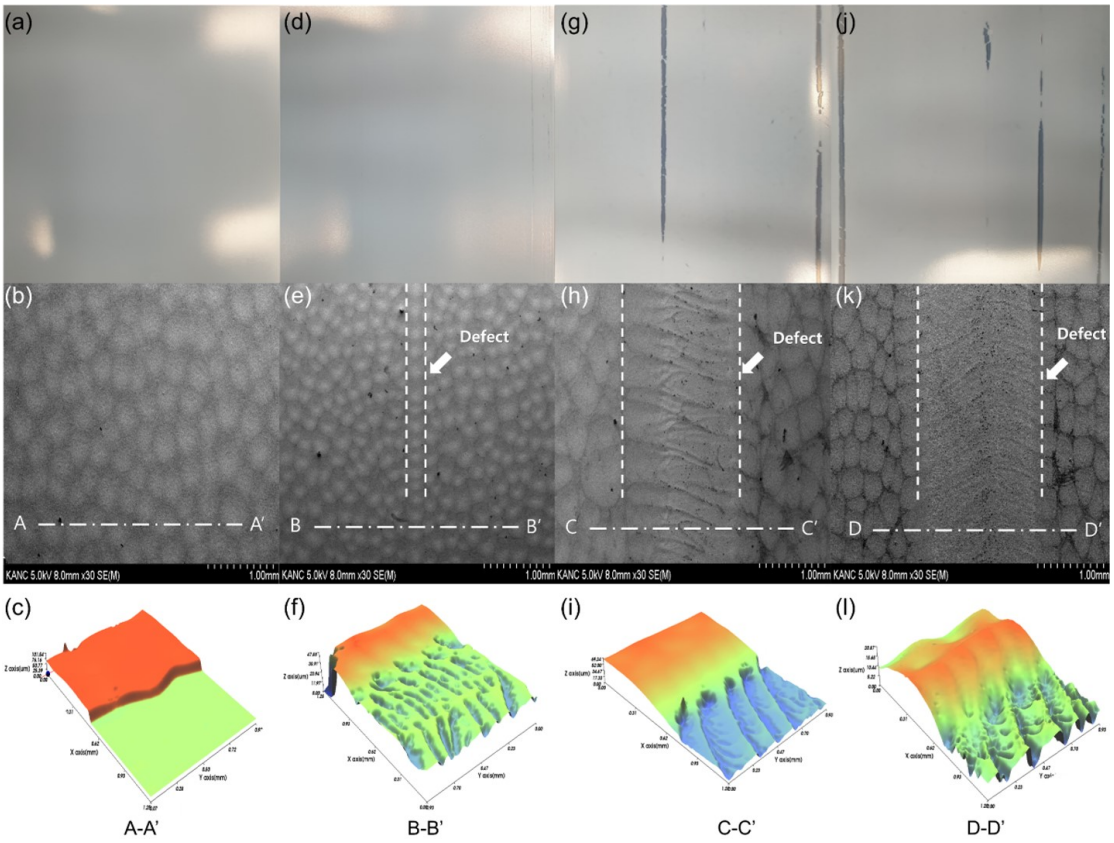


**Figure 8.** Surface and SEM, interferometer image of YSZ coating layer dried at (a-c) 30°C, (d-f) 60°C, (g-i) 90°C, and (j-l) 120°C.

The effects of the coating defects on the performance of the SOFC were experimentally analyzed. SOFCs were fabricated using the YSZ layers fabricated at different drying temperatures shown in Figure 8. The open circuit voltages (OCV), which directly affect the internal resistance and performance of SOFCs, were measured. Equation (2) presents the mathematical model of OCV obtained using Nernst equation [26].

$$E_T = E_0 + \frac{RT}{2F} ln(P_{H_2}) - \frac{RT}{2F} ln(P_{H_2O}) + \frac{RT}{2F} ln(P_{O_2}^{\frac{1}{2}}) \quad (2)$$

where ET represents the OCV, $R$ is the universal gas constant (8.314 $JK^{-1}mol^{-1}$), $T$ and $F$ are the temperature and Faraday constant (96,484 $Cmol^{-1}$), respectively; $P_{H_2}$, $P_{H_2O}$ and $P_{O_2}$ are the partial pressures of $H_2$, $H_2O$ and $O_2$ at 1 atm, respectively.

Figure 9 indicates the OCV measurement of the SOFCs fabricated using the YSZ layer at 30, 60, 90, and 120 °C drying temperatures. It is clearly seen that the OCV using the YSZ layer fabricated at 60, 90, and 120 °C cannot be measured due to the coating defects. This means that the coating defects due to the web unevenness could damage the SOFC and decrease its yield in the R2R process. These results suggest that the effects of the web unevenness on the coating defect due to convection and conduction heats from the dryer should be considered in the fabrication of the brittle electrolyte using the R2R process. For instance, one can determine the distance between the slot-die coater and the inlet of the dryer considering the minimum permissible distance at which web unevenness is not generated by considering the web unevenness according to the distance between the position of the slot-die coater and dryer inlet at the drying temperature set by user.

Preprints (www.preprints.org) | NOT PEER-REVIEWED | Posted: 18 November 2020 doi:10.20944/preprints202011.0465.v1

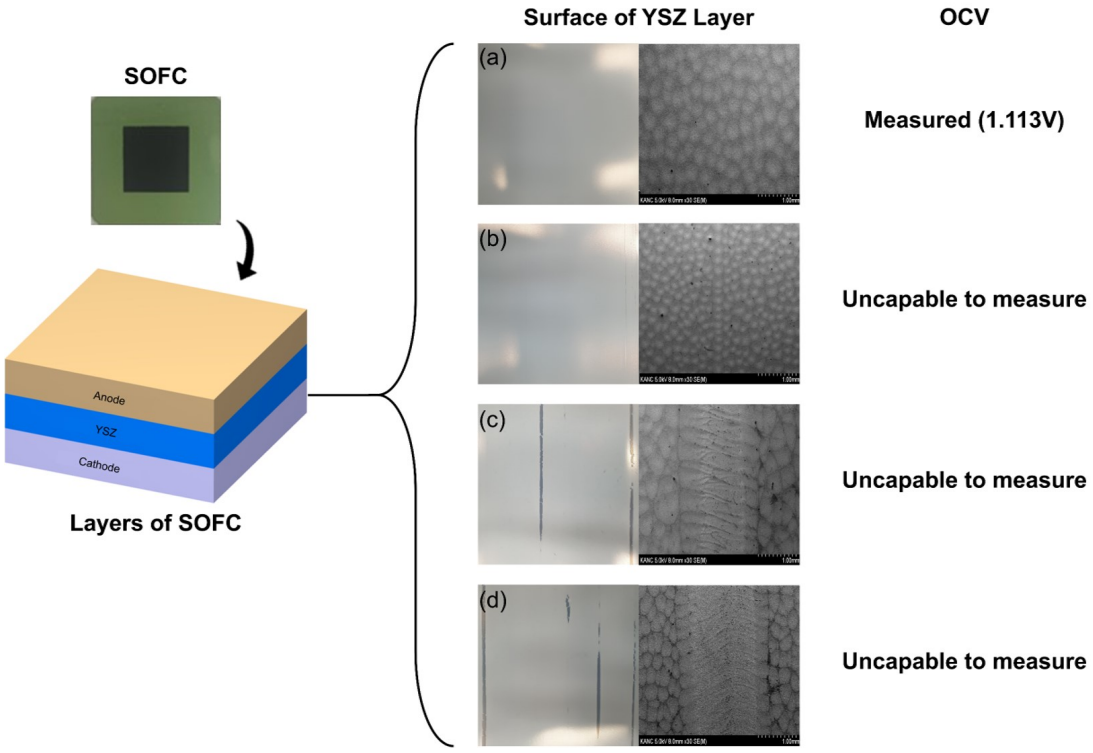


**Figure 9.** OCV of SOFC fabricated at (a) 30°C, (b) 60°C, (c) 90°C, and (d) 120°C.

## 4. Conclusion

In this study, we analyzed the effects of thermally-deformed web unevenness on the coating quality of the brittle electrolyte layer. First, the effect of the conduction and convection heats from the dryer on the deformation of the tensioned web were analyzed according to the drying temperature using FEA. We found that the web unevenness can be generated by thermal deformation due to the conduction and convection heats from the dryer, but the amplitudes and positions of the peaks and valleys of the unevenness wave form change when the web moves in the dryer. The amplitude of the web unevenness increases with increasing the drying temperature, and the web unevenness in the dryer eventually spreads to the coating section. The YSZ layers were coated according to the drying temperature to clearly observe the effect of the web unevenness on the coating defects. Experimental results indicate that the web unevenness at the coating section can generate the coating defect in x-direction, which could damage the SOFC. This study suggests that the coating defect generated by the web unevenness owing to the convection and conduction heats from the dryer should be considered in the fabrication of brittle electrolytes using the R2R process. Results of this study can be useful when designing the R2R process for the mass production of large-area SOFCs.

**Author Contributions:** Conceptualization, M.J. and C.L.; data curation, S.K.; Formal Analysis, M.J. and S.K.; writing—original draft preparation, M.J. and C.L.; supervision, J.L. and C.L.; project administration, C.L.; Writing-Review & Editing J.L. and C.L.; Funding Acquisition, C.L. All authors have read and agreed to the published version of the manuscript.

**Funding:** Please add: This work was supported by a National Research Foundation of Korea (NRF) grant funded by the Korea government (MIST) (No.2020R1A2C1012428) & (No.2020R1A5A1019649).

**Conflicts of Interest:** The authors declare that they have no known competing financial interests or personal relationships that could have appeared to influence the work reported in this paper.

## References


1. Larsen-Olsen, T.T.; Andersen, T.R.; Andreasen, B.; Böttiger, A.P.L.; Bundgaard, E.; Norrman, K.; Andreasen, J.W.; Jørgensen, M.; Krebs, F.C. Roll-to-roll processed polymer tandem solar cells partially processed from water. *Sol. Energy mater Sol. Cells*. **2012**, *97*, 43-49.
2. Lee, J.; Byeon, J.; Lee, C. Theories and Control Technologies for Web Handling in the Roll-to-Roll Manufacturing Process. *Int. J. Precis. Eng. Manuf. Green Technol.* **2020**, *7*, 525–544.
3. Ma, L.; Chen, J.; Tang, W.; Yin, Z. Transverse vibration and instability of axially travelling web subjected to non-homogeneous tension. *Int. J. Mech. Sci* **2017**, *133*, 752-758.
4. Lee, J.; Kim, S.; Lee, C. Taper tension profile in roll-to-roll rewinder: Improving adhesive force of pressure-sensitive adhesive film. *Int. J. Precis. Eng. Manuf. Green Technol*. **2019**, *6*, 853–860.
5. Kang, H.; Lee, C. Optimal design of pneumatic flotation for roll-to-roll conveyance in the production of printed circuits. *Appl. Sci.* **2020**, *10.16*, 5440.
6. Lee, J.; Byeon, J.; Lee, C. Fabrication of thickness-controllable double layer electrolyte using roll-to-roll additive manufacturing system. *Int. J. Precis. Eng. Manuf. Green Technol.* **2020**, *7*, 635–642.
7. Lee, J.; Kim, S.; Lee, C. Surface drying for brittle material coating without crack defects in large-area roll-to-roll coating system. *Int. J. Precis. Eng. Manuf. Green Technol.* **2019**, *6*, 723–730.
8. Xia, Z. C.; Hutchinson, J. W. Crack patterns in thin flms. *J. Mech. Phys. Solids*. **2020,** *48.6-7*, 1107–1131.
9. Ebler, N. A.; Arnason, R.; Michaelis, G.; D'Sa, N. Tension control: Dancer rolls or load cells. *IEEE Trans. Ind. Appl.* **1993**, *29.4*, 727-739.
10. Park, J.; Kim, D.; Lee, C. Contact angle control of sessile drops on a tensioned web. *Appl. Surf. Sci.* **2018**, *437*, 329-335.
11. Mollamahmutoglu, C.; Good, J.K. Modeling the influence of web thickness and length imperfections resulting from manufacturing processes on wound roll stresses. *CIRP J. Manuf. Sci. Technol.* **2015**, *8*, 22-33.
12. Chen, Z.; Zheng, Y.; Zhou, M.; Wong, D. S. H.; Chen, L.; Deng, Z; Model-based feedforward register control of roll-to-roll web printing systems. *Control. Eng. Pract.* **2016**, *51*, 58-68.
13. Sakamoto, T.; Fujino, Y. Modelling and analysis of a web tension control system. *Proc. of the IEEE Int. Symposium* **1995**, *1*, 358-362.
14. Lynch, A. F.; Bortoff, S. A.; Röbenack, K. Nonlinear tension observers for web machines. *Automatica (Oxf)* **2004**, *40.9*, 1517-1524.
15. Shin, K. H.; Kwon, S. O. The effect of tension on the lateral dynamics and control of a moving web. *IEEE Trans. Ind. Appl.* **2007**, *43.2*, 403-411.
16. Lee, C.; Kang, H.; Kim, C.; Shin, K. A novel method to guarantee the specified thickness and surface roughness of the roll-to-roll printed patterns using the tension of a moving substrate. *J. Microelectromech. Syst.* **2010**, *19.5*, 1243-1253.
17. Lee, J.; Shin, K.; Lee, C. Analysis of dynamic thermal characteristic of register of roll-to-roll multi-layer printing systems. *Robot. Comput. Integr. Manuf.* **2015**, *35*, 77-83.
18. Lu, Y.; Pagilla, P. R. Modeling of temperature distribution in a moving web transported over a heat transfer roller. Dynamic Systems and Control Conference. Fort Lauderdale, Florida, USA, October 17-19, 2012.
19. Park, J.; Kim, S.; Lee, C. An analysis of pinned edge layer of slot-die coated film in roll-to-roll green manufacturing system. *Int. J. Precis. Eng. Manuf. Green Technol.* **2018,** *5.2*, 247-254.
20. Lee, J.; Kim, S.; Lee, C. Large area electrolyte coating through surface and interface engineering in roll-to-roll slot-die coating process. *J. Ind. Eng. Chem.* **2019,** *76*, 443-449.
21. Kang, Y.; Jeon, Y.; Ji, H.; Kwon, S.; Kim, G. E.; Lee, M. G. Optimizing roller design to improve web strain uniformity in roll-to-roll process. *Appl. Sci.* **2020,** *10.21*, 7564.
22. Gao, H.; Liu, J.; Chen, H.; Li, S.; He, T.; Ji, Y.; Zhang, J. The effect of Fe doping on the properties of SOFC electrolyte YSZ. *Solid State Ion* **2008,** *179.27-32*, 1620-1624.
23. Saebea, D.; Authayanun, S.; Patcharavorachot, Y.; Chatrattanawet, N.; Arpornwichanop, A. Electrochemical performance assessment of low-temperature solid oxide fuel cell with YSZ-based and SDC-based electrolytes. *Int. J. Hydrog. Energy* **2018**, *43.2*, 921-931.
24. Spiridigliozzi, L.; Di Bartolomeo, E.; Dell'Agli, G.; Zurlo, F. GDC-Based infiltrated electrodes for solid oxide electrolyzer cells (SOECs). *Appl. Sci.* **2020**, *10.11*, 3882.

25. Irshad, M.; Siraj, K.; Raza, R.; Ali, A.; Tiwari, P.; Zhu, B.; Rafique, A.; Ali, A.; Ullah, M.K.; Usman, A. A brief description of high temperature solid oxide fuel cell's operation, materials, design, fabrication technologies and performance. *Appl. Sci.* **2016**, *6.3*, 75.
26. Chiodelli, G.; Malavasi, L. Electrochemical open circuit voltage (OCV) characterization of SOFC materials. *Ionics (Kiel)*, **2013**, *19.8*, 1135-1144.